Two-stage oxygen delivery for enhanced radiotherapy by perfluorocarbon nanoparticles

Zaigang Zhou[1,2], Baoli Zhang[1,2], Haoran Wang[1,2], Ahu Yuan[1,2,*], Yiqiao Hu[1,2,3,*], Jinhui Wu[1,2,3,*]

Affiliations:

[1] State Key Laboratory of Pharmaceutical Biotechnology, Medical School of Nanjing University & School of Life Sciences, Nanjing University, Nanjing 210093, China

[2] Institute of Drug R&D, Nanjing University, Nanjing 210093, China

[3] Jiangsu Provincial Key Laboratory for Nano Technology, Nanjing University, Nanjing 210093, China

[*] **Author for correspondence:**

Jinhui Wu, Ph.D.

Address: 22 Hankou Road, Nanjing University, Nanjing 210093, China

Phone: +86-25-83596143

Fax: +86-25-83596143

E-mail: wuj@nju.edu.cn

Yiqiao Hu, Ph. D

Address: 22 Hankou Road, Nanjing University, Nanjing 210093, China

Phone: +86-25-83596143

Fax: +86-25-83596143

E-mail: huyiqiao@nju.edu.cn

Ahu Yuan, Ph. D

Address: 22 Hankou Road, Nanjing University, Nanjing 210093, China

Phone: +86-25-83596143

Fax: +86-25-83596143

E-mail: yuannju@163.com

Supporting Methods:

Synthesis of PFC@HSA nanoparticles

Generally, HSA (96 mg) and DTT were firstly mixed in 2.4 mL deionized water followed by stirring for 10 min. Then, 200 μL alcohol was added followed by shaking for another 3 min. PFTBA (0.6 mL), Perfluoroocytlbromide (PFOB) (0.6 mL), Perfluorotripropylamine (PFTPA) (0.48 mL) and Perfluorodecalin (FDC) (0.12 mL) or Perfluoro-N-methylcyclohexylpiperidineand (FMCP) (0.48 mL) and FDC (0.12 mL) were added gradually to the solution in an ice bath under at 300 W sonication for 6 min to form stable PFC@HSA nanoparticles.

Effects of PFC@HSAs on platelets function

Platelet preparation

Blood of Balb /C male mice was collected into tubes containing sodium citrate as anticoagulant. Then, blood was centrifuged at 203 g for 8 min, and PRP (platelet-rich plasma) was collected into a fresh tube. PRP was further centrifuged at 1028 g for 5 min after addition of PGI2 (125 ng/mL). Platelets (4×10^8 cells/mL) were finally re-suspended in modified Tyrodes-Hepes buffer (134 mM NaCl, 2.9 mM KCl, 0.34 mM $Na_2HPO_4.12H_2O$, 12 mM $NaHCO_3$, 20 mM Hepes and 1 mM $MgCl_2$, pH 7.3).

Clot retraction

PRP was prepared as previously described. 200 μL mouse PRP was firstly mixed with 50 μL Vehicle (32mg/mL HSA) or 50 μL PFC@HSAs. Then, the solution was raised to 1mL with modified Tyrodes-Hepes buffer, and then 5 μL of red blood cells were added. Fibrin clot formation was initiated by adding 5 μL thrombin (200 U/mL). Clot retraction around a glass capillary added before clot formation was observed over a period of 90 min at room temperature. Blood clot weight and extruded serum weight were measured as markers of blood clot retraction.

Effects of PFTBA@HSA on tumor cell and normal cells

Generally, 10^4 HUVEC (Human umbilical vein endothelial cell), Raw 264.7 (bone marrow derived macrophage), CT26 tumor cells or 4T1 cells in DMEM culture medium were seeded into 96-well plate. Three hours later, different concentrations of PFTBA@HSA were added and cultured for another 24 h. Then, cell viability was qualitatively examined using CCK-8 assay. For CCK-8 based cell activity assay, a mixed solution consisted of CCK-8 (10 μL) and fresh culture medium (90 μL) was added to each well, followed by incubating for additional 1 h. Finally, the absorbance was measured at 450 nm using a microplate reader.

NIR Fluorescence Imaging of IR775 loaded PFTBA@HSA

CT26 tumors bearing Balb/C mice were used for *in vivo* NIR fluorescence imaging. IR775-labeled PFTBA@HSA (0.4 mg/kg IR775, 20% PFTBA) was intravenous injected when the tumor reached approximately 200 mm^3. Fluorescent images of mice were obtained at 1 h, 10 h, 24 h, 48 h and 72 h by the CRI Master System. After 72 h, the mice were finally killed by euthanasia. Then, tumors and other major tissues were collected and subjected to *ex vivo* NIR fluorescence imaging.

Tumor vessel permeation assay

For Evans Blue permeation assay, mice were intravenously injected with 10 mL/kg different PFTBA@HSA or Vehicle. 5 h later, Evans Blue (40 mg/kg) was injected intravenously. The mice were sacrificed and tumors were collected after another 3 h. One part of the tumors was embedded in OCT (Sakura, Japan) and cut into 8 μm slices. The immunofluorescence images of the slices were observed by confocal microscope (Nikon, Japan).

For Dextran (2000 kDa) permeation assay, mice were firstly intravenously injected with 10 mL/kg PFTBA@HSA or Vehicle. 5 h later, Dextran (40 mg/kg) was injected intravenously. The mice were sacrificed and tumors were collected after another 3 h. One part of the tumors was embedded in OCT (Sakura, Japan) and cut into 8 μm slices. The immunofluorescence images of the slices were observed

by confocal microscope (Nikon, Japan).

Effects of PFTBA@HSA on RBCs infiltration

RBCs infiltration in tumor was detected by hemoglobin detection, tumors were firstly excised from the sacrificed animals. Then, the tumors were weighed and homogenized in Drabkin's reagent (Sigma) followed by centrifuging at 15000 g for 10 min. The hemoglobin content of supernatants was measured by absorbance at 540 nm.

Effects of PFTBA@HSA on *in situ* tumor metastasis

Generally, Balb/C mice bearing subcutaneous 4T1 tumors (~100 mm^3) were randomly divided into four groups (n=5): (a) Vehicle (32 mg/mL HSA, 10 mL/kg); (b) PFTBA@HSA (10 mL/kg); These drugs were given at day 0, day 3 and day 7. At day 14, the *in situ* tumors were removed and the wound sites were sewn with thread. Finally, the lung metastases were calculated after another 24 days.

Effects of PFTBA@HSA on TGF-β Activation

To detect the TGF-β in serum, mice were divided into three groups (n=5): (a) Vehicle (32 mg/mL HSA, 10 mL/kg); (b) PFTBA@HSA (10 mL/kg); (c) Ticagrelor (10 mg/kg). 10 h later, the mice were sacrificed and the blood were collected. Then, the latent and active TGF-β were detected by Elisa Kit (Dakewe, China).

Statistical Analysis

Data are presented as mean ± SD. Statistical analysis was performed via one-way ANOVA. Meanwhile, post hoc analysis was performed using the Wilcoxon rank sum test with a Bonferroni correction if needed. *$p<0.05$ was considered statistically significant, and **$p<0.01$ and ***$p<0.001$ were extremely significant.

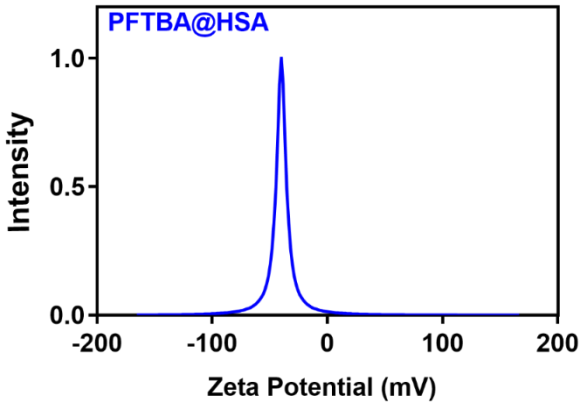

Figure S1. Zeta Potential curve of PFTBA@HSA.

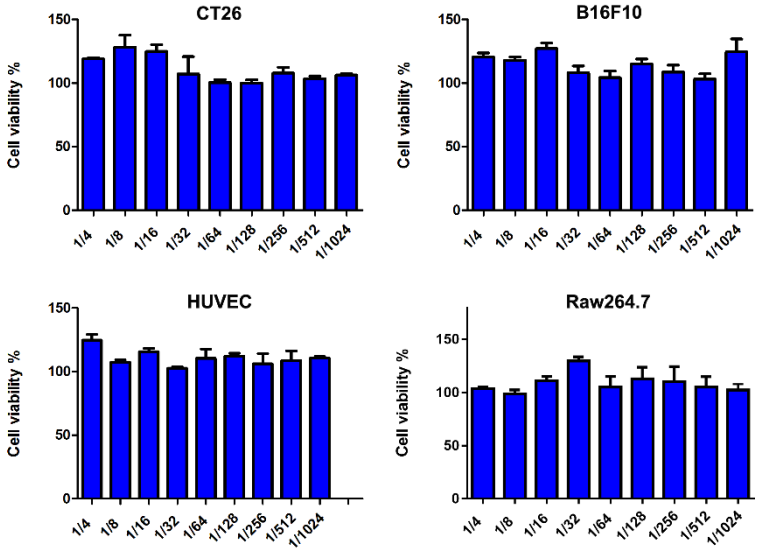

Figure S2. Cell toxicity of PFTBA@HSA on normal cells and tumor cells after different dilution rates (n=6). Data are shown as the mean ± SD. Statistical analysis was performed via one-way ANOVA test.

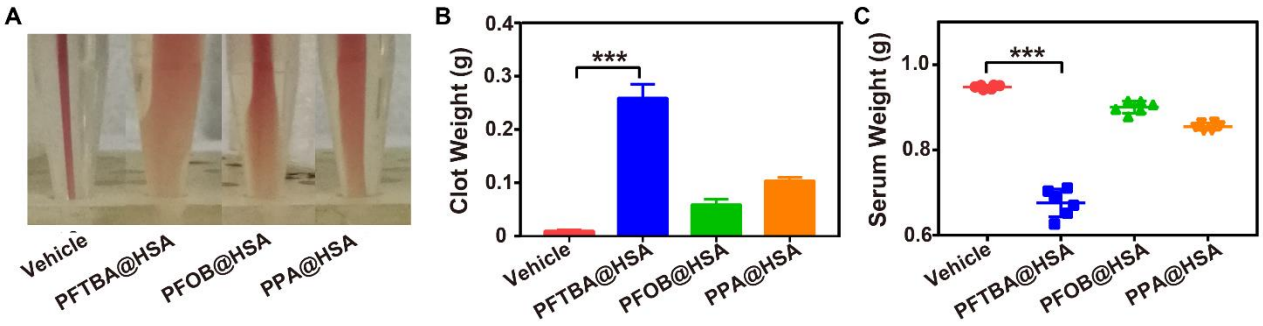

Figure S3. Effects of PFC@HSAs on platelets inhibition. (A) Representative image of blood retraction after different PFC@HSAs treatments. (B) Quantification of serum weight (n=6). (C) Quantification of clotting weight (n=6). Data are shown as the mean ± SD. Statistical analysis was performed via one-way ANOVA test. ***p<0.001.

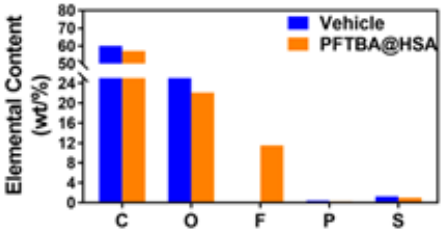

Figure S4. Possible mechanism of PFTBA@HSA medicated platelet inhibition. The elemental contents after PFTBA@HSA or Vehicle treatment. Results showed that PFTBA@HSA may absorb on the platelets.

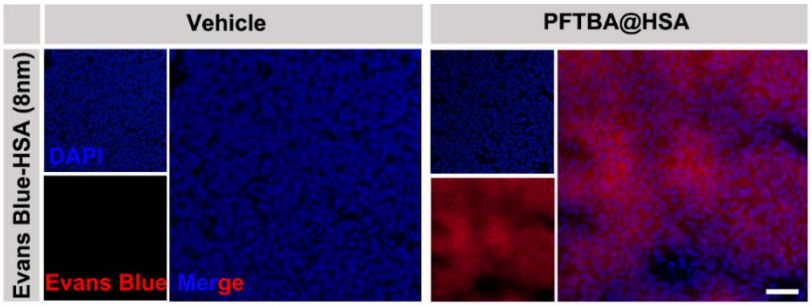

Figure S5. Representative fluorescence images of tumor tissues after intravenous injection of Evans Blue, scale bar=50 μm

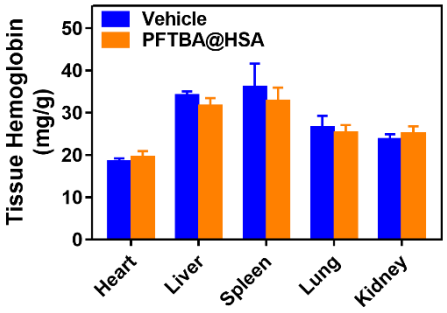

Figure S6. Quantification of hemoglobin at 10 h after PFTBA@HSA or Vehicle treatment. Data are shown as the mean ± SD. Statistical analysis was performed via one-way ANOVA test.

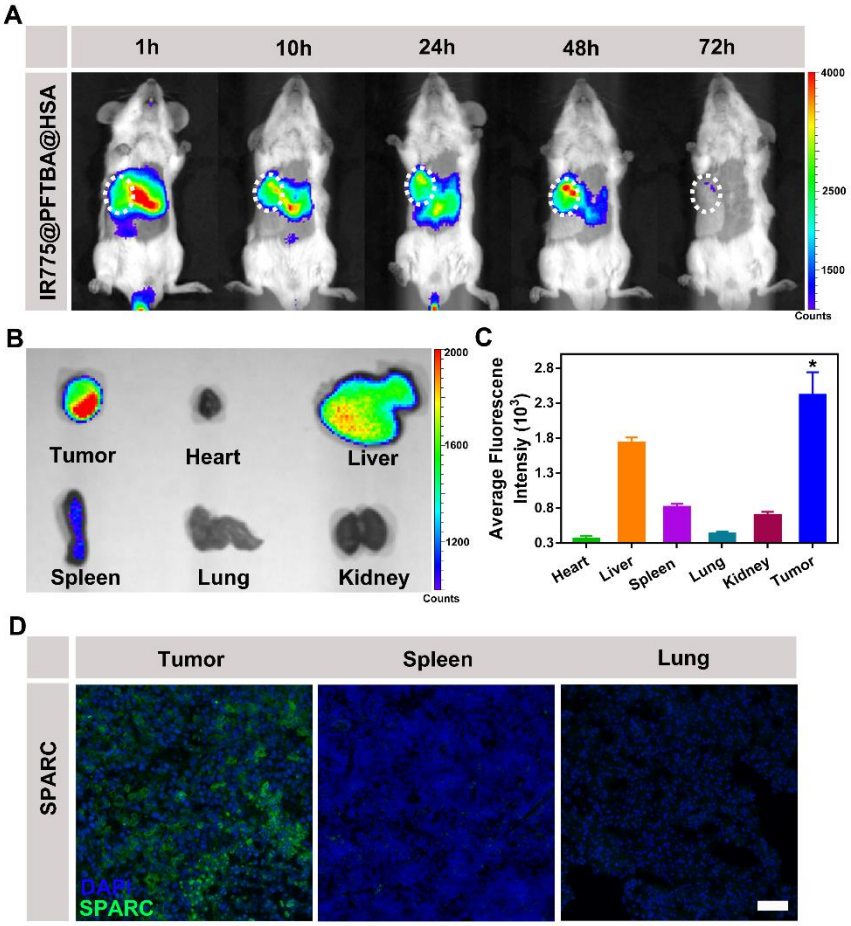

Figure S7. The active tumor targeting ability of PFTBA@HSA. (A-B) *In vivo* dynamic fluorescence imaging after IR775 loaded PFTBA@HSA injection and *ex vivo* fluorescence images of major organs and tumors at 72 h post treatment. White circles indicate the location of tumors. (C) Quantification of PFTBA@HSA in the tumor and other tissues by the IR775 fluorescence at 72 h post-treatment. (D) Representative SPARC fluorescence staining images of tumor slices and normal tissue slices, scale

bar=50 μm. Data are shown as the mean ± SD. Statistical analysis was performed via one-way ANOVA test. *p<0.05.

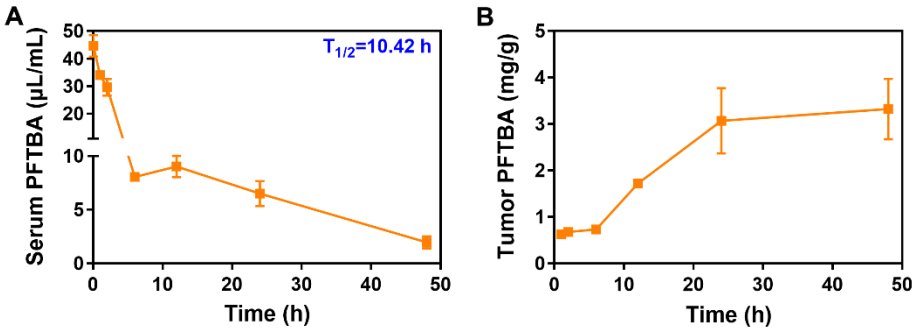

Figure S8. (A) Blood circulation of PFTBA@HSA determined by GC (n=3). (B) Dynamic distribution PFTBA in tumor after intravenous injection of PFTBA@HSA determined by GC (n=3). Data are shown as the mean ± SD.

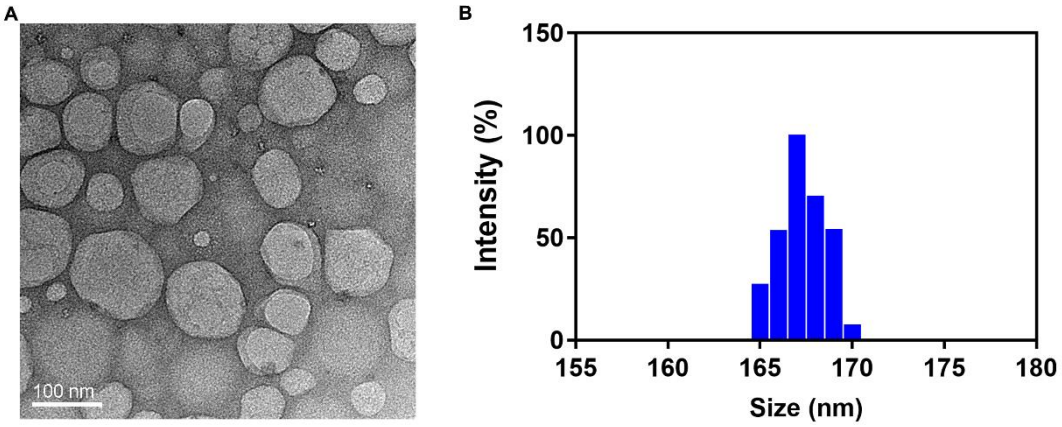

Figure S9. Synthesis and characteristics of PPA@HSA. (A) TEM images of PPA@HSA, scale bar=100 nm. (B) Diameters of PPA@HSA detected via dynamic light scattering.

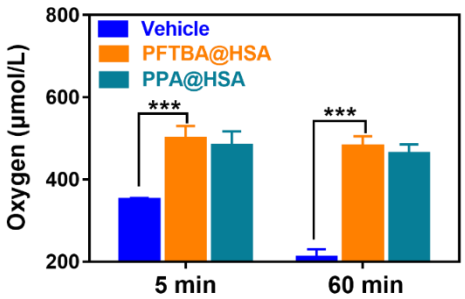

Figure S10. The oxygen binding ability of PFC@HSAs under 1 atmospheric pressure. Data are shown

as the mean ± SD. Statistical analysis was performed via one-way ANOVA test. ***p<0.001.

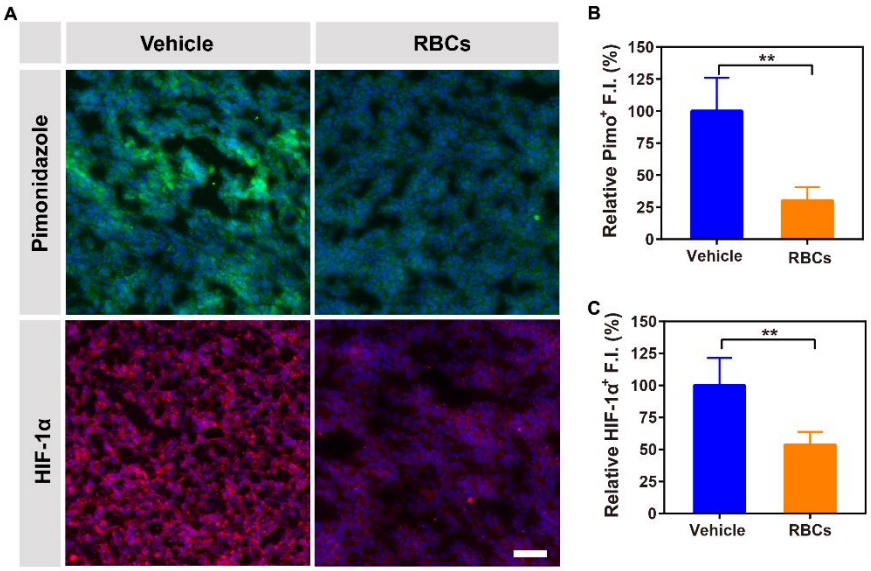

Figure S11. (A) Representative immunofluorescence images of tumor slices stained with the hypoxia probe Pimonidazole or HIF-1α at 12 h after intratumoral injection of 10 μL red blood cells or Vehicle; scale bar=100 μm. (B-C) Quantification of relative HIF-1α or Pimonidzole fluorescence intensity at 12 h after treatments (n=3). Data are shown as the mean ± SD. Statistical analysis was performed via one-way ANOVA test. **p<0.01.

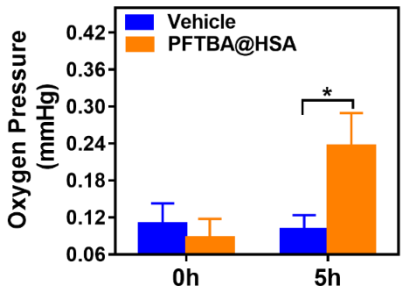

Figure S12. Quantification of the oxygen concentration in the CT26 tumor detected by Oxylite™ oxygen probe (n=7). Data are shown as the mean ± SD. Statistical analysis was performed via one-way ANOVA test. *p<0.05.

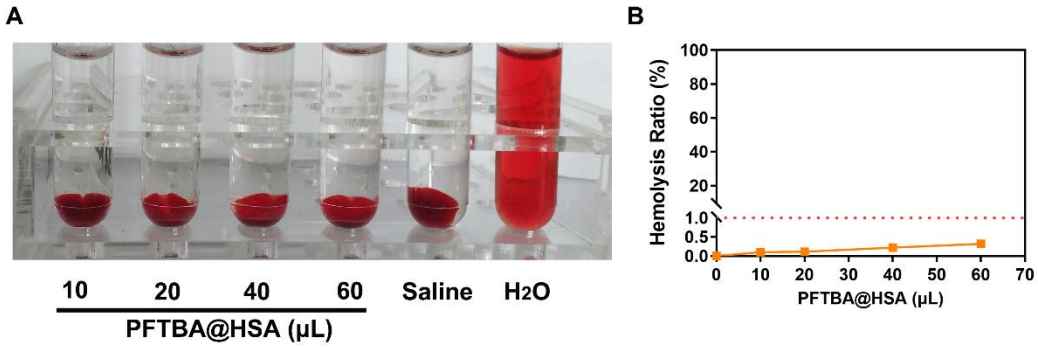

Figure S13. Hemolytic effect of PFTBA@HSA. (A) Image of each experimental group. Red blood cells dissolved in saline were set as negative control while red blood cell dissolved in water were set as positive control. (B) Hemolytic rate induced by PFTBA@HSA at different concentration. Data are shown as the mean ± SD. Statistical analysis was performed via one-way ANOVA test.

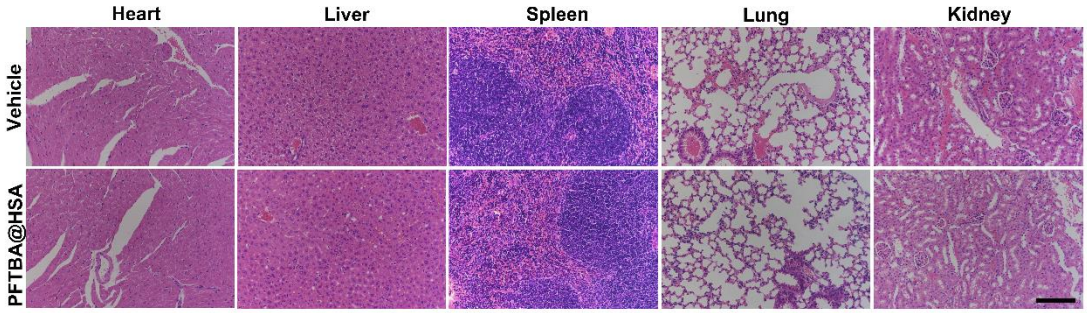

Figure S14. H&E staining of PFTBA@HSA treated normal tissue slices at Day 1 (short-term tissue toxicity) post PFTBA@HSA treatment. No obvious tissue toxicity was visible in all normal tissues, scale bar=100 μm.

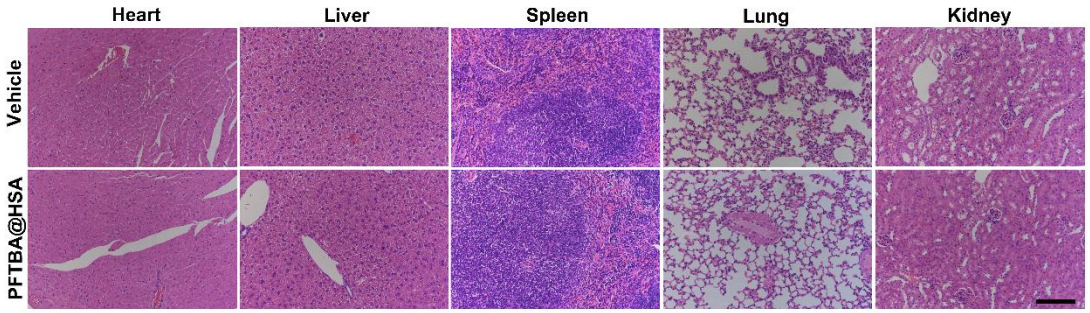

Figure S15. H&E staining of PFTBA@HSA treated normal tissue slices at Day 7 (long-term tissue toxicity) post PFTBA@HSA treatment. No obvious tissue toxicity was visible in all normal tissues, scale bar=100 μm.

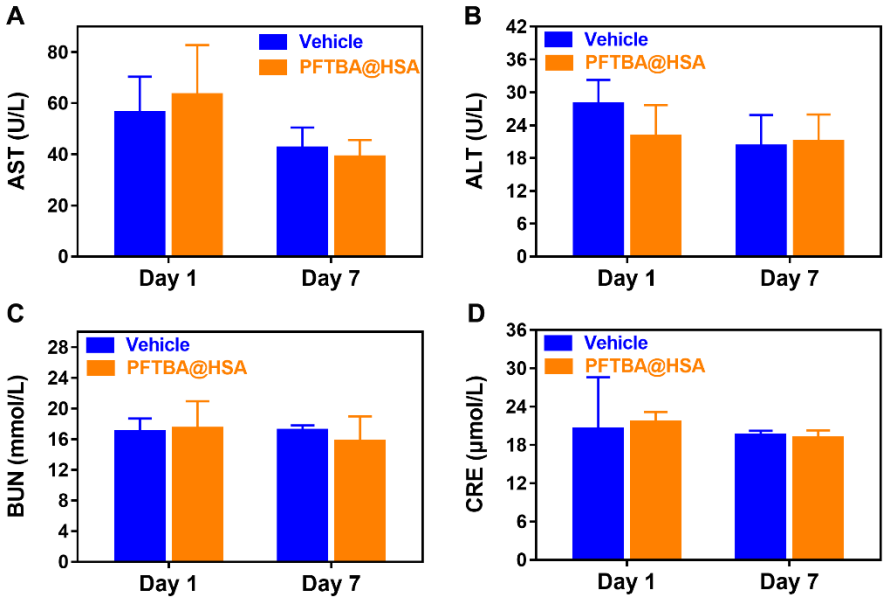

Figure S16. (A-B) Serum biochemistry data reflecting liver function including aspartate aminotransferase (AST) and alanine aminotransferase (ALT); (C-D) Serum biochemistry data reflecting kidney function including blood urea nitrogen (BUN) and creatinine (Cre). Data are shown as the mean ± SD. Statistical analysis was performed via one-way ANOVA test.

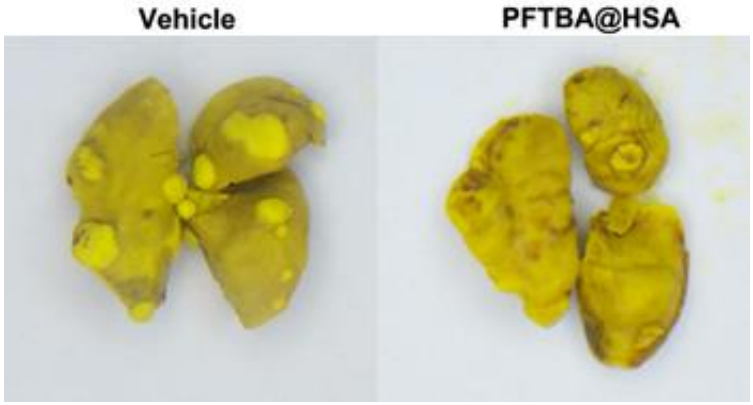

Figure S17. Representative photos of lung metastases at day 24 after removing *in situ* 4T1 tumor

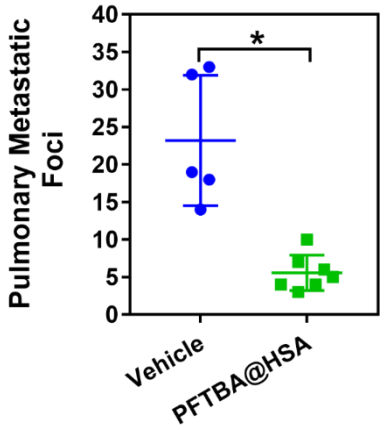

Figure S18. Quantification of the total numbers of visible lung metastases 24 days after removing *in situ* 4T1 tumors. Data are shown as the mean ± SD. Statistical analysis was performed via Wilcoxon rank sum test. *p<0.05.

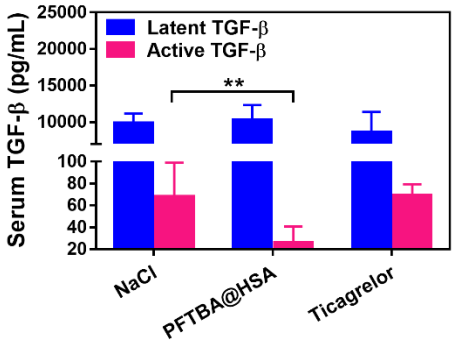

Figure S19. Quantification of the latent and active serum TGF-β at 12 h by Elisa Kit. Data were shown as the mean±SD. Statistical analysis was performed via one-way ANOVA test. **p<0.01.